Arteriosclerosis, Thrombosis, and Vascular Biology

BASIC SCIENCES

Neutrophil Extracellular Trap Degradation by Differently Polarized Macrophage Subsets

Patrick Haider, Julia B. Kral-Pointner, Julia Mayer, Manuela Richter, Christoph Kaun, Christine Brostjan, Wolf Eilenberg, Michael B. Fischer, Walter S. Speidl, Christian Hengstenberg, Kurt Huber, Johann Wojta, Philipp Hohensinner

OBJECTIVE: Macrophages are immune cells, capable to remodel the extracellular matrix, which can harbor extracellular DNA incorporated into neutrophil extracellular traps (NETs). To study the breakdown of NETs we studied the capability of macrophage subsets to degrade these structures in vitro and in vivo in a murine thrombosis model. Furthermore, we analyzed human abdominal aortic aneurysm samples in support of our in vitro and in vivo results.

APPROACH AND RESULTS: Macrophages were seeded onto blood clots or isolated NETs and polarized. All macrophages were capable to degrade NETs. For initial breakdown, macrophages relied on extracellular deoxyribonucleases. Proinflammatory polarization enhanced NET degradation. The boost in degradation was because of increased macropinocytosis, as inhibition by imipramine diminished their NET breakdown. Inhibition of macropinocytosis in a murine thrombosis model led to increased NET burden and reduced thrombus resolution in vivo. When analyzing abdominal aortic aneurysm samples, macrophage density furthermore corresponded negatively with the amount of local NETs in the intraluminal thrombi as well as in the vessel wall, as increased macrophage density was associated with a reduction in NET burden.

CONCLUSIONS: We provide evidence that macrophages degrade NETs by extracellular predigestion and subsequent uptake. Furthermore, we show that proinflammatory macrophages increase NET degradation through enhanced macropinocytosis, priming them for NET engulfment. Based on our findings, that inhibition of macropinocytosis in mice corresponded to increased NET amounts in thrombi and that local macrophage density in human abdominal aortic aneurysm is negatively associated with surrounding NETs, we hypothesize, that macrophages are able to degrade NETs in vivo.

GRAPHIC ABSTRACT: A graphic abstract is available for this article.

Key Words: aortic aneurysm ■ extracellular traps ■ humans ■ macrophages ■ thrombosis

Macrophages are important effector cells in tissue repair as well as in the resolution of inflammation.[1] They form a heterogeneous population of phagocytic cells, distributed throughout the body, which can be recruited to sites of inflammation by cytokines and chemokines.[2] With their repertoire of different receptors found not only on the cell surface (eg, IL [interleukin] receptors and chemokine receptors) but also in their cytoplasm (eg, hormone receptors and toll-like receptors), macrophages can sense the environment and polarize into different subsets, leading to the adaption of the cells to actual needs of the organism.[2–4] In vivo, macrophages display often mixed phenotypes, depending on the encountered stimuli and tissue.[5] For in vitro studies, macrophage polarization can be induced by specific stimuli.[6] Proinflammatory macrophage polarization is achieved by lipopolysaccharide and IFN-γ (interferon-γ) stimulation, alternative macrophage polarization is simulated in vitro via the cytokines IL-4 and IL-13. Polarization leads to changes in macrophage

See accompanying editorial on page 1961
See cover image

Correspondence to: Johann Wojta, PhD, Medical University of Vienna Waehringer Guertel 18-20, 1090 Vienna, Austria. Email johann.wojta@meduniwien.ac.at

The Data Supplement is available with this article at https://www.ahajournals.org/doi/suppl/10.1161/ATVBAHA.120.314883.

For Sources of Funding and Disclosures, see page 2276.

Nonstandard Abbreviations and Acronyms

AAA	abdominal aortic aneurysm
citH4	citrullinated histone H4
DNase	deoxyribonuclease
IFN-γ	interferon γ
IL-13	interleukin 13
IL-4	interleukin 4
MPO	myeloperoxidase
NETs	neutrophil extracellular traps
ROI	regions of interest

function, including different migratory behavior or altered extracellular matrix remodeling as we and others have shown before.[7–11] This plasticity allows macrophages to adapt to the environmental needs by altering their ability to produce specific signal proteins[12] or to take up dead cells, debris,[13] and extracellular DNA.[14]

In recent years, a special form of extracellular DNA deposition called neutrophil extracellular traps (NETs) was identified. NETs were first described by Brinkmann et al[15] as mechanism of neutrophils to trap bacteria in a network of DNA. These NETs are studded with neutrophil-derived enzymes, leading to bacterial killing. However, NETs, by providing a scaffold for platelets and coagulatory proteins also support thrombus formation.[16–18] Recently, it was shown that extracellular histones, which are part of NETs, are able to induce lytic cell death of smooth muscle cells in an atherosclerotic mouse model, indicating a destabilizing role of NETs in chronic vascular diseases.[19] In abdominal aortic aneurysms (AAAs), NETs promote inflammation which leads to the recruitment of inflammatory cells to the vessel wall. The recruited cells release proteolytic enzymes, leading to medial remodeling and thinning, ultimately resulting in aortic dilatation and rupture. Conversely, NET inhibition attenuates macrophage infiltration and leads to reduced disease development,[20] prompting them as potential therapeutic targets in AAA and several other diseases as reviewed recently.[21]

Although many studies have been exploring the generation and pathophysiology of NETs, knowledge on their degradation and the restitution of tissues is scarce. Overall, deoxyribonuclease (DNase) activity is required to prevent spontaneous formation of intravascular thrombi containing NETs,[22] showing that a counterbalance of NET generation and degradation is necessary for the maintenance of proper homeostasis. Macrophages have been described as being capable of degrading NETs in vitro,[23–25] however, data on the impact of polarization of macrophages on their NET-degrading ability and in vivo evidence for this notion are lacking so far.

The aim of our study was to determine the capacity of macrophages to degrade NETs and to identify the endocytic pathway, to investigate whether polarization would change the kinetics of uptake and degradation both in vitro and in vivo.

Highlights

- Macrophages preprocess extracellular DNA derived from neutrophil extracellular traps (NETs) by deoxyribonucleases.
- Uptake of NETs through phagocytosis is necessary for their degradation by macrophages.
- Proinflammatory polarization of macrophages enhances their ability to degrade NETs by additional utilization of macropinocytosis.
- In a mouse model of thrombosis, inhibition of macropinocytosis leads to increased NETs in the thrombus and reduced resolution of the thrombus.
- In human abdominal aortic aneurysm, local macrophage density is negatively associated with NET amounts.

We show here that macrophages degrade NETs by an interplay of extracellular and secreted DNases followed by intracellular uptake. Furthermore, we provide evidence that proinflammatory polarization of macrophages can boost NET degradation by increased utilization of macropinocytosis. Inhibition of macropinocytosis in an in vivo thrombosis mouse model led to increased NET burden in the thrombi and concomitant decreased thrombus resolution. In addition, we demonstrate that local macrophage density in human AAA samples is negatively associated with surrounding NETs, further supporting our hypothesis that macrophages are key modulators of extracellular DNA degradation.

MATERIALS AND METHODS

The data that support the findings of this study are available from the corresponding author upon reasonable request. Please see the Major Resources Table in the Data Supplement for all used materials. Detailed methods' descriptions are available in the Methods in the Data Supplement.

Ethical Approval

Blood samples from healthy human donors, as well as human AAA samples, were obtained after written informed consent was given, and studies were performed according to recommendations of the ethical board of the Medical University of Vienna (1575/2014 and 1729/2014). All animal procedures were approved by the animal ethical board of the Medical University of Vienna and the Austrian Federal Ministry of Education, Science and Research (BMBWF-66.009/0258-WF/V/3b/2017).

In Vitro Generation and Polarization of Macrophages

Macrophages were generated from human monocytes, which were isolated from blood samples of apparently healthy volunteers and polarized with lipopolysaccharide and IFN-γ or IL-4 and IL-13, respectively, as published previously.[10] In total,

macrophages from 84 volunteers were used in this study. Macrophage generation and characterization are described in detail in the Methods in the Data Supplement and are also shown in Figure I in the Data Supplement. All inhibitors used with macrophages were confirmed to be nonapoptotic (Figure II in the Data Supplement).

Blood Clot Formation In Vitro

Blood clots were generated as published before[26] and put into Tissue-Tek O.C.T. (Scigen). Details are provided in the Methods in the Data Supplement. Frozen samples were cut on a cryomicrotome (Leica) and used as described below.

Murine Vena Cava Thrombosis Model

The murine vena cava thrombosis model was performed as described by Brill et al.[27] Before surgery, all mice were treated intraperitoneally with a mixture of medetomidine, midazolam, fentanyl, and ketamine to achieve analgesia and anesthesia and subsequently, analgesia was continued for the whole time of experiment using buprenorphine. The detailed protocol, exact concentrations and application routes of drugs, sample size calculation and drug dosage calculation[28] are provided in the Methods in the Data Supplement.

Immunofluorescent Staining of In Vitro Generated Blood Clots, Mouse Thrombi, and Human AAA Specimens

Staining was performed on acetone-fixed frozen sections of blood clots or mouse thrombi. The detailed protocol, used antibodies, and concentrations are given in the Methods in the Data Supplement. Fluorescence images were acquired on TissueFAXS microscope (TissueGnostics) using a 20x Zeiss air objective.

Uptake of NETs From Blood Clots by Polarized Macrophages

Macrophages at 1×10^6 cells were seeded onto unfixed sections of blood clots, polarized, and incubated for 2 hours at 37°C in a humidified atmosphere and fixed with 4% formaldehyde afterwards. Immunohistochemical staining of the sections was performed using a rabbit anti-citrullinated histone 4 (citH4, 2 µg/mL, Merck) antibody and anti-rabbit horseradish peroxidase-DAB Cell & Tissue Staining Kit (R&D systems). Slides were processed as suggested by the manufacturer, nuclei were counterstained with Mayer's hematoxylin (Sigma-Aldrich) and mounted using Eukitt mounting medium (Sigma-Aldrich). Bright-field images of citH4 uptake were acquired with TissueFAXS microscope (TissueGnostics) using a 20x Zeiss air objective. Uptake of NETs by macrophages was defined as cytoplasmatic signal of citH4 and quantified by blinded counting cytoplasmic citH4 negative and positive cells in 10 randomly chosen 500×500 µm sized regions of interest (ROI) of each macrophage subset and donor, respectively.

Flow Cytometric Measurement of DNA Uptake From Blood Clots by Macrophages

DNA content of in vitro generated clots was stained with 1 µmol/L SytoxGreen (ThermoFisher) diluted in Hanks' Balanced Salt Solution (Corning). The slides were washed extensively, and 1×10^6 macrophages were seeded onto the slides in RPMI 1640 (Sigma-Aldrich) supplemented with 10% fetal bovine serum (Millipore) as well as penicillin, streptomycin, fungizone, glutamine (Lonza) and incubated for 2 hours at 37°C in a humidified atmosphere. Afterwards, the cells were scratched, fixed in 4% formaldehyde and treated 30 minutes with 4 mU/mL DNase 1 (Promega) at 37°C to digest all membrane-bound DNA. Analysis was done by flow cytometry on an Attune NxT flow cytometer (ThermoFisher), and macrophages were identified by their forward and sideward scatter properties.

NET Generation

Neutrophil granulocytes were isolated from human blood using the EasySep Direct Human Neutrophil Isolation Kit (Stemcell). Neutrophils at 1×10^5 cells were seeded in Hanks' Balanced Salt Solution (Corning) containing 100 nmol/L phorbol 12-myristate 13-acetate (Sigma-Aldrich) and 1 µmol/L Sytox Green (ThermoFisher) into LabTek 8 chamber slides (ThermoFisher) and incubated for 4 hours at 37°C in a humidified atmosphere to generate fluorescence-labeled NETs. NETs were stored at 4°C before use.

Degradation of NETs In Vitro

Macrophages at 1×10^4 cells were added to wells containing NETs generated as described above, polarized, and incubated for 24 hours at 37°C in a humidified atmosphere. RPMI 1640 only and DNase 1 (4 mU/mL, Promega) in RPMI 1640 were added as negative (NETs only) and positive controls (DNase 1). Total NET amount per well was quantified at given time points by acquiring fluorescent images with the TissueFAXS microscope (TissueGnostics) using a 2.5x Zeiss air objective and NET area in each individual well was calculated using FIJI image analysis software.[29] Relative NET amount compared with time point 0 was calculated for each well and time point. The relative amount of each well at each time point was then normalized towards the relative NET amount of the NETs only control. As indicated in the respective NET degradation experiments, macrophages were treated with 1 µg/mL cytochalasin D (Abcam), 10 mmol/L ammonium chloride (Sigma-Aldrich), 5 µmol/L imipramine hydrochloride (Sigma-Aldrich), or 5 mmol/L EDTA (Sigma-Aldrich), respectively. All NET degradation experiments, except the ones testing imipramine or supernatants, were performed simultaneously to rule out interindividual variance in degradation kinetics.

Protein Quantification

DNases were quantified using Human DNase 1 ELISA Kit (Nordic BioSite AB), Human DNase 1L3 ELISA Kit (Abbexa Ltd), and Human DNase 2A ELISA Kit (MyBioSource Inc) as indicated by the manufacturer's instructions.

DNase 1L1 protein was quantified by flow cytometry using a rabbit anti-DNase 1L1 antibody (10 µg/mL, Atlas Antibodies), which was detected by an anti-rabbit Alexa647-conjugated secondary antibody (5 µg/mL, Biolegend).

For the detection of TREX 1 (three prime repair exonuclease 1) as well as DNase 1:actin complexes, custom-made ELISAs were used using 2 different TREX 1 antibodies (0.2 µg/mL, ThermoFisher; 0.6 µg/mL, horseradish peroxidase conjugated,

Santa Cruz) or a DNase 1 (0.2 µg/mL, ThermoFisher) and an actin antibody (0.6 µg/mL, Abcam) as published previously.[30] Details are provided in the Methods in the Data Supplement.

Immunofluorescent Staining of DNase 1L1

DNase 1L1 staining was performed on macrophages polarized for 6 or 24 hours. Samples were blocked with 2% BSA, 0.5% fish gelatine, and 0.3% Tween20 in PBS (Morphisto) and afterwards incubated with a rabbit anti-DNase 1L1 antibody (0.2 µg/mL, Atlas Antibodies). Detection was performed using an anti-rabbit Cy3 antibody (2.5 µg/mL, Biolegend). Actin cytoskeleton as well as nuclei were stained with phalloidin-iFluor488 (1:1000, Abcam) and DAPI (1 µg/mL, Sigma-Aldrich). The slides were mounted with Aqueous Mounting Medium (Abcam). Fluorescence images were acquired on a Zeiss LSM 700 confocal microscope using a Zeiss 63x oil objective and a pinhole of 1 airy unit (≈0.8 µm slice thickness).

Quantification of Macrophages and NETs in Tissue Samples

Samples were stained as described before. The whole region of each sample was acquired on TissueFAXS microscope (TissueGnostics) using 20x Zeiss air objective. Total amounts of citH4 and macrophages in each sample, identified as CD68 or F4/80+ cells, were counted using FIJI and expressed as relative citH4 area or macrophage count per mm^2. For the quantification of local NETs surrounding macrophages in thrombi, 5 200×200 µm sized ROIs were acquired per specimen, and the relative citH4 positive area was calculated using FIJI. The average of these 5 regions per mouse was compared between the 2 groups. In AAA nine 200×200 µm sized ROIs were acquired per specimen and classified for macrophage content. $CD68^{low}$ regions were defined as <5 macrophages per ROI, $CD68^{medium}$ had 5 to 10 macrophages per ROI and $CD68^{high}$ regions showed >10 macrophages per ROI. The percentage of NET area of each ROI was calculated in FIJI by calculating the sum of pixels of the NET fluorescence channel divided through total pixel amount of each ROI.

Apoptosis Assessment

Apoptosis was assessed by flow cytometric AnnexinV staining of macrophages treated for 24 hours with different inhibitors used in the respective experiments. For a detailed description see the Methods in the Data Supplement.

RNA Extraction, Quantitative Polymerase Chain Reaction, and DNA Electrophoresis

RNA extraction as well as quantitative polymerase chain reaction were performed as published previously.[31] Primer sequences are given in Table I in the Data Supplement. For a detailed description see the Methods in the Data Supplement.

Isotype Controls for Immunostaining

Appropriate isotype antibodies were used as a control for all immunohistochemical and immunofluorescent stainings. The respective images are shown in Figure III in the Data Supplement.

Statistical Analysis

Statistical analysis was performed in GraphPad Prism 8. Normality was assessed using D'Agostino-Pearson test (n≥8) or Shapiro-Wilk test (n<8). For normally distributed data an unpaired or paired *t* test was calculated comparing 2 groups, or 1-way ANOVA was performed for >2 groups. Non-normally distributed data were assessed with the Mann-Whitney test for 2 groups, or, if >2 groups were compared, the Kruskal-Wallis test for unpaired data or Friedman test for paired data was used, respectively. If >1 parameter was analyzed 2-way ANOVA was performed. Correction for multiple testing was done by controlling the false discovery rate with the 2-stage linear step-up procedure of Benjamini, Krieger, and Yekutieli. The used tests are stated in each of the respective subfigures' legend.

RESULTS

NETs Form Spontaneously in Human Clotting Blood

To study the capacity of macrophages to degrade extracellular DNA, blood clots were generated in vitro. When we stained these clots, we found large areas of the clot covered by NETs, which were identified as structures positive for citH4, myeloperoxidase, CD177, and DAPI (Figure 1A and 1B).

Uptake of NETs Through Differently Polarized Macrophages

We examined the capability to degrade NETs and subsequently take up DNA from in vitro generated blood clots in unpolarized, proinflammatory M(lipopolysaccharide+IFN-γ) and alternatively activated M(IL-4+IL-13) macrophages. All macrophage subsets were able to ingest NETs but interestingly, ≈2-fold more M(lipopolysaccharide+IFN-γ) stained positive for citH4 in their cytoplasm compared with unpolarized M0 or M(IL-4+IL-13) (Figure 1C). We confirmed our results by flow cytometry using SytoxGreen-labeled DNA in blood clots. Macrophages were able to take up labeled DNA (Figure 1D) and proinflammatory polarization of macrophages enhanced the uptake of labeled DNA (Figure 1E).

Degradation of In Vitro Generated NETs by Differently Polarized Macrophages

To characterize the kinetics of NET degradation by differently polarized macrophages, we investigated the breakdown of NETs by macrophages in vitro. As can be seen from Figure 2A, 1×10^4 macrophages degraded significantly more NETs when they were polarized into proinflammatory M(lipopolysaccharide+IFN-γ) after seeding as compared to M(IL-4+IL-13) or M0, respectively. EDTA is a chelator of the divalent ions Ca^{2+}, Mg^{2+},

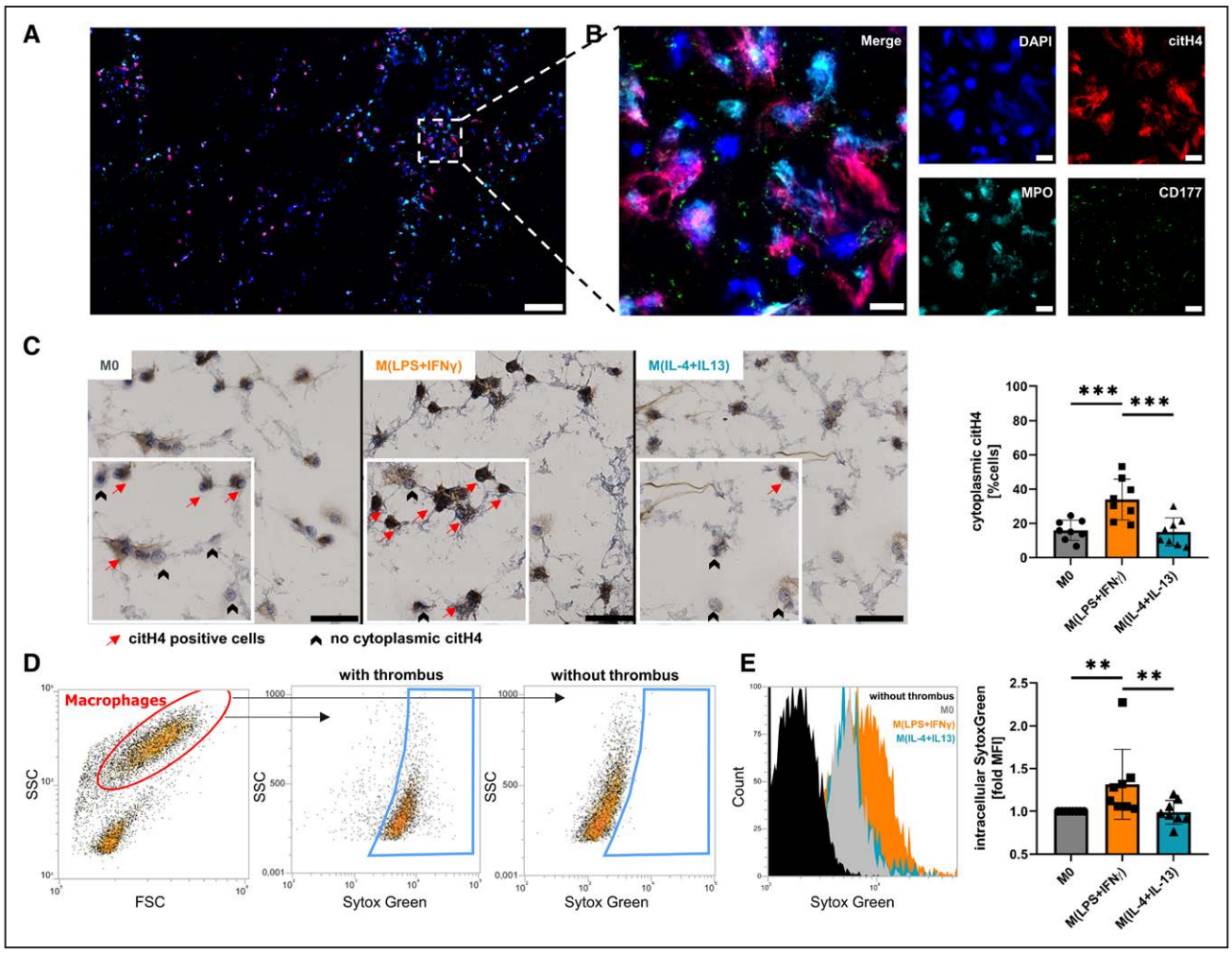

Figure 1. Macrophages take up DNA and neutrophil extracellular traps (NETs) from in vitro generated blood clots.
A, Spontaneous NET formation was visualized by immunofluorescent staining of citrullinated histone 4 (citH4), myeloperoxidase (MPO), and CD177 (×20 magnification, scale bar 200 µm). **B**, Magnification of the marked area in (**A**; scale bar 20 µm). **C**, Macrophage subsets were seeded onto blood clots, and cytoplasmic citH4 was quantified after 2 h by immunohistochemical staining. A zoomed area from each picture is shown in the canvas. Data represent mean±SD (×20 magnification, scale bar 50 µm; n=8, D'Agostino-Pearson test, 1-way ANOVA with Benjamini-Krieger-Yekutieli false discovery rate). **D**, Differently polarized macrophages were incubated for 2 h on SytoxGreen-labeled clots, and DNA uptake was analyzed by fluorescence-activated cell sorting. Representative fluorescence-activated cell sorting plot of DNA uptake. **E**, Quantification of **D**. An overlay of histograms is shown **left**. Data represent mean±SD of fold change to M0 (n=8, D'Agostino-Pearson test, Friedman test for non-normally distributed paired data with Benjamini-Krieger-Yekutieli false discovery rate). $^{**}P<0.01$ and $^{***}P<0.001$.

Mn^{2+} which are essential for DNases to exert their enzymatic activity.[32,33] As can be seen from Figure 2B, 5 mmol/L EDTA reduced the breakdown of NETs by ≈80% as compared to conditions without EDTA.

In Vitro Generated Macrophages Produce and Secrete DNase 1L3

To further examine if secreted DNases could be responsible for the breakdown of NETs, conditioned medium from macrophages, which were differently polarized for 24 hours was tested. Conditioned medium alone, collected from 1×10^4 macrophages after 24 hours was not capable to degrade NETs over a 24 hours observational period, whereas higher concentrated conditioned medium from 2.5×10^5 macrophages induced NET breakdown, which was inhibited by the addition of 5 mmol/L EDTA (Figure IVA in the Data Supplement). However, no difference in degradation kinetics between medium of differently polarized macrophages was seen. We confirmed the presence of DNase activity in the conditioned medium of 24 hours polarized macrophage subsets (Figure IVB in the Data Supplement) and similarly no difference between the subsets was observed. In humans, 2 DNases are secreted, namely DNase 1 and DNase 1L3. Although all macrophage subsets expressed mRNA specific for DNase 1 as well as DNase 1L3 (Figure VA in the Data Supplement), DNase 1 protein levels in the supernatant from polarized and unpolarized macrophages were below detection limit of the used ELISA (data not shown) and only DNase 1L3 levels in the supernatant

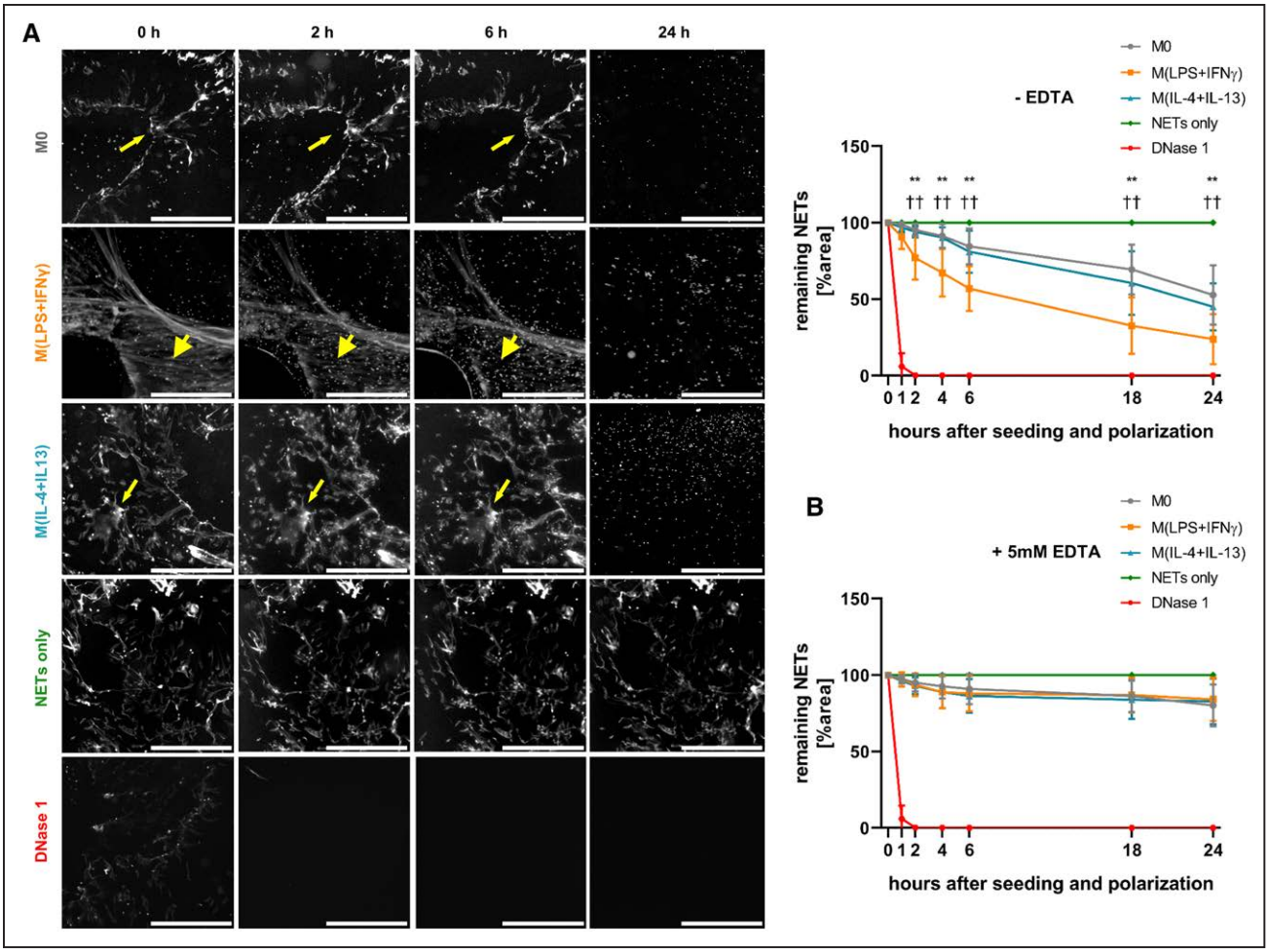

Figure 2. Degradation of in vitro generated neutrophil extracellular traps (NETs) by differently polarized macrophages. **A**, NETs were generated in vitro and labeled fluorescently, 1×10^4 macrophages were seeded onto the NET layer, polarized and the extent of remaining NETs was quantified at different time points. Values are given in percent remaining NET area in comparison to time point 0 and are normalized towards a control without cells (NETs only). Four mU/mL deoxyribonuclease (DNase) 1 was used as positive control and added at time point 0. M(lipopolysaccharide [LPS]+IFN [interferon]-γ) significantly faster degraded the NET layer (thick arrowheads) compared with the other 2 subsets, which did not differ in their NET degradation capacity (thin arrowheads; ×2.5 magnification, scale bar 50 µm). Data represent mean±SD (n=8, 2-way ANOVA for different time points with Benjamini-Krieger-Yekutieli false discovery rate). **B**, NETs were generated as in **A** and 1×10^4 macrophages were seeded in the presence of 5 mmol/L EDTA onto them, polarized and remaining NETs were quantified as in **A** (scale bar 50 µm). Data represent mean±SD (n=8) $^{**}P<0.01$ between M0 and M(lipopolysaccharide [LPS]+IFN-γ); $\dagger\dagger P<0.01$ between M(lipopolysaccharide [LPS]+IFN-γ) and M(IL-4+IL-13).

were detectable. No significant differences in levels of DNase 1L3 secreted by polarized or unpolarized macrophages, respectively, were seen (Figure IVC in the Data Supplement).

Characterization of Intracellular DNases in Human Macrophage Subsets

As the differences in early NET degradation by differently polarized macrophages could not be explained by respective differences in the levels of secreted DNases in our experiments, we quantified the intracellular DNases DNase 1, DNase 1L1, DNase 1L3, DNase 2, and TREX 1. After 6 hours of polarization, however, no differences in mRNA (Figure VB in the Data Supplement) and protein amounts of these DNases were observed between the individual subsets of macrophages (Figure 3A). Long-term polarization for 24 hours led to a significant increase in protein amounts of intracellular DNase 1 in M(lipopolysaccharide+IFN-γ) as compared to M0 and alternatively polarized M(IL-4+IL-13). DNase 2 was significantly increased in polarized M(lipopolysaccharide+IFN-γ) and M(IL-4+IL-13), compared with unpolarized M0 after 24 hours (Figure 3A). As cytoplasmic DNase 1 is bound to actin,[34] we measured DNase 1:actin complexes after 24 hours in cell lysates of polarized macrophages. M(lipopolysaccharide+IFN-γ) displayed increased intracellular DNase1:actin complexes, compared with the other 2 subsets (Figure 3B). For intracellular DNase 1L1, DNase 1L3, and TREX 1, we did not observe any significant differences after 6 and 24 hours of polarization. It is known that polarization may alter the amount and protein distribution on the filopodia of macrophages and that this spatial

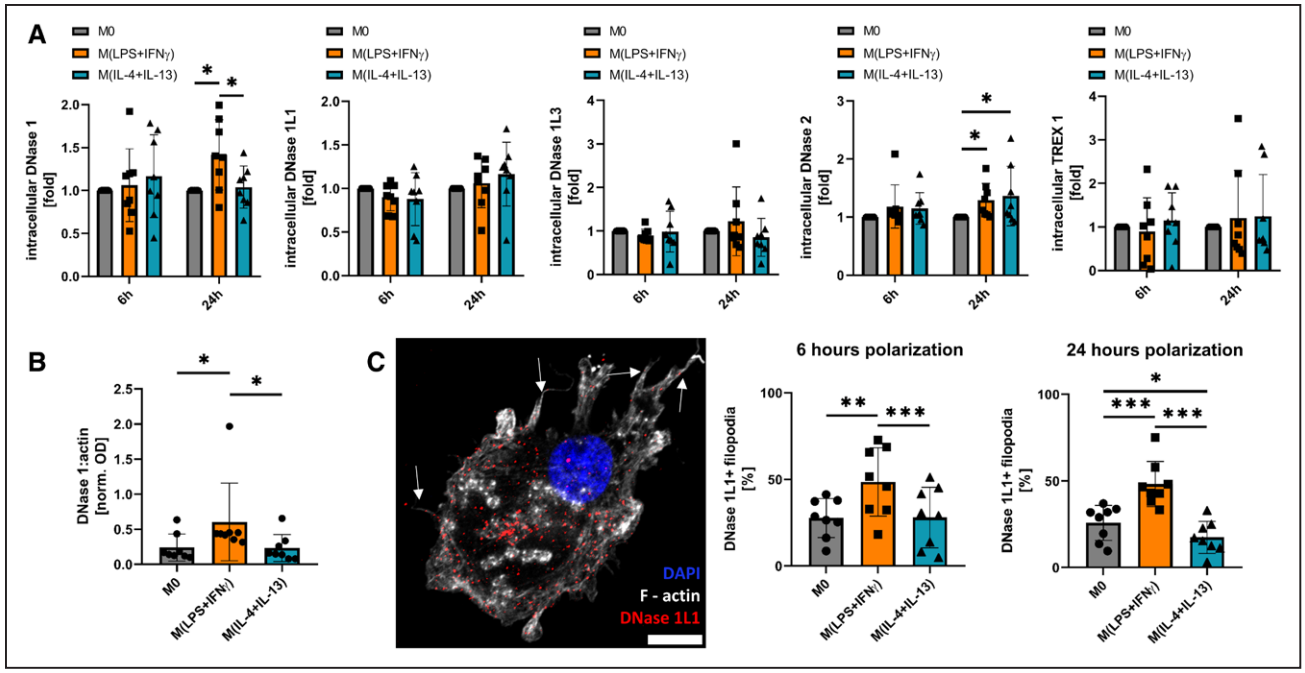

Figure 3. Characterization of intracellular deoxyribonucleases (DNases).
A, Intracellular DNases in polarized macrophages were quantified as described in the Materials and Methods section. Data are given as fold compared with M0 and represent mean±SD (n=8, 2-way ANOVA for different time points with Benjamini-Krieger-Yekutieli false discovery rate). **B**, Intracellular DNase 1:actin complexes were analyzed by a custom-made ELISA. Data are given as normalized OD of each sample and represent mean±SD (n=8, D'Agostino-Pearson test, Friedman test for non-normally distributed paired values with Benjamini-Krieger-Yekutieli false discovery rate). **C**, Fluorescence microscopy of surface DNase 1L1 in macrophages polarized for 6 or 24 h. On the left side, a representative picture of a 6 h polarized M(lipopolysaccharide [LPS]+IFN [interferon]-γ) macrophage is shown with arrows pointing to DNase 1L1 positive filopodia. Data are expressed as percent DNase 1L1 positive filopodia and represent mean±SD (×63 magnification, scale bar 10 μm; n=8, D'Agostino-Pearson test, 1-way ANOVA with Benjamini-Krieger-Yekutieli false discovery rate). **P*<0.05, ***P*<0.01, and ****P*<0.001.

relocalization could influence matrix degradation through defined mobilization of enzymes to the cell membrane.[35] DNase 1L1 is the only known DNase with a membrane-anchoring ability through a glycosylphosphatidylinositol-anchor.[36] Immunofluorescent staining of DNase 1L1 colocalization to filopodia revealed increased amounts of filopodia staining positive for DNase 1L1 in M(lipopolysaccharide+IFN-γ), which were polarized for 6 or 24 hours (Figure 3C). When macrophages were polarized for 24 hours before seeding the cells onto NETs, no difference in the NET breakdown by the differently polarized macrophages was seen (Figure VIA in the Data Supplement).

Mechanism of NET Uptake by Differently Polarized Macrophages

To further characterize the mechanism of NET uptake and degradation by macrophages, individual components of endocytosis were blocked. Actin polymerization was inhibited by treating the cells with 1 μg/mL of cytochalasin D,[37] before seeding the cells onto the NET layer. Breakdown of NETs by all macrophage subsets was almost completely abolished by cytochalasin D (Figure VIB in the Data Supplement). Similarly, treatment of macrophages with 10 mmol/L ammonium chloride, which inhibits phagosome-lysosome fusion,[38] did also prevent the degradation of NETs (Figure VIC in the Data Supplement).

Treatment of cells with 5 μmol/L imipramine, an inhibitor of macropinocytosis,[39] significantly reduced breakdown of NETs by M(lipopolysaccharide+IFN-γ) after 6 and 24 hours as compared to untreated M(lipopolysaccharide+IFN-γ). In contrast, imipramine did not affect the degradation of NETs by M0 or M(IL-4+IL-13) significantly (Figure 4A and 4B). Macropinocytosis was significantly increased after 2 hours in M(lipopolysaccharide+IFN-γ) shortly after stimulation with cytokines and subsequently dropped to about 50% of baseline levels after 24 hours polarization, which was assessed by fluorescent dextran uptake (Figure VID in the Data Supplement). Withdrawal of lipopolysaccharide+IFN-γ for 1 hour before the analysis of dextran uptake did not change macropinocytosis rate significantly, revealing an initial priming for enhanced macropinocytosis through lipopolysaccharide+IFN-γ, without the need of continuous stimulation (Figure VID in the Data Supplement).

Inhibition of Macropinocytosis in an In Vivo Murine Thrombosis Model Leads to Increased Thrombus NET Burden and Reduced Thrombus Resolution

Stenosis of the inferior vena cava leading to thrombus formation was induced in twelve 8 to 12–weeks-old female C57BL/6 mice by inferior vena cava ligature surgery. Six

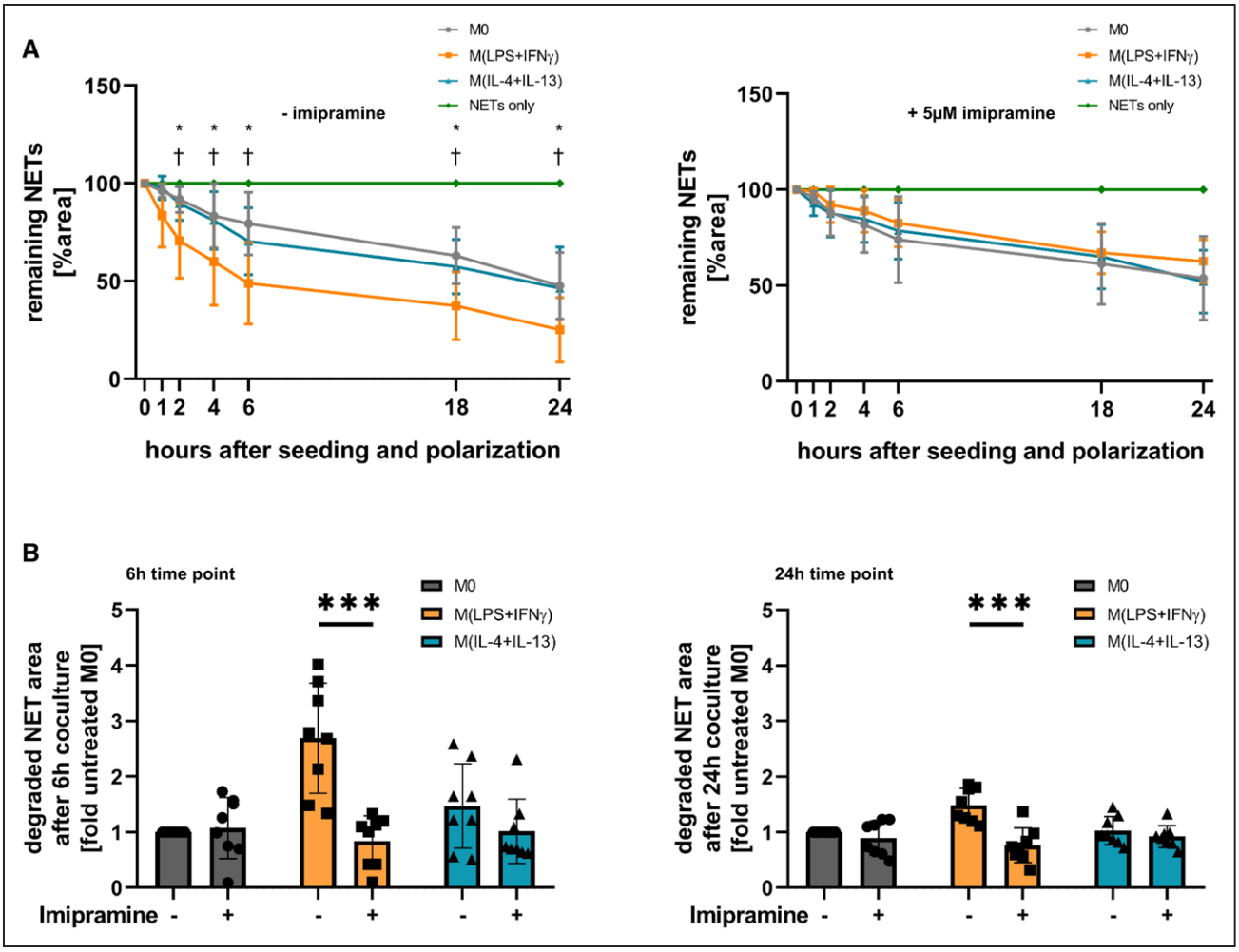

Figure 4. Increased neutrophil extracellular trap (NET) degradation by M(lipopolysaccharide [LPS]+IFN [interferon]-γ) is dependent on macropinocytosis.

A, Macrophages were either untreated (**left**) or treated with 5 µmol/L imipramine (**right**) for 30 min, seeded onto a NET layer and polarized. Degradation was measured at the indicated time points after seeding and the extent of remaining NETs was quantified at these time points. Values are given in percent remaining NET area in comparison to time point 0, normalized towards a control without cells (NETs only). Data represent mean±SD (n=8, 2-way ANOVA with Benjamini-Krieger-Yekutieli false discovery rate) *P<0.05 between M0 and M(lipopolysaccharide [LPS]+IFN-γ); †P<0.05 between M(lipopolysaccharide [LPS]+IFN-γ) and M(IL-4+IL-13). **B**, The remaining NET area at 6 and 24 h is shown from the experiment in **A,** and data are plotted for each donor as fold to untreated M0 macrophages (n=8, 2-way ANOVA with Benjamini-Krieger-Yekutieli false discovery rate). ***P<0.001.

mice each were then assigned randomly to either a control or an imipramine group. After 1 week, mice were euthanized, and the thrombi were harvested together with the inferior vena cava. The experimental setup and baseline characteristics are shown in Figure VII in the Data Supplement. Thrombus length as well as diameter were significantly increased in mice treated with imipramine after 1 week (Figure 5A and 5B). To rule out a reduced infiltration of the thrombi by imipramine treatment, we stained the thrombi for F4/80$^+$ macrophages. No statistically significant difference was observed between the 2 groups (Figure 5C, P=0.28). In mice treated with imipramine, NET burden, identified as structures positive for citH4, myeloperoxidase, Ly6G, and DAPI, was significantly higher than in the control group 7 days after thrombus formation (Figure 5D). To characterize the relative location of NETs and macrophages in the thrombi, five 200×200 µm sized randomly selected macrophage-rich ROIs, identified by high F4/80 signal, were analyzed for their relative citH4+ area. There was significantly more citH4 signal around macrophages in the imipramine group compared with the control group (Figure 5E).

Local Macrophage Density Is Inversely Associated With Surrounding NETs in Human Abdominal Aortic Aneurysms

Human AAA samples have been reported to contain NETs.[40] To investigate NET degradation by macrophages in human tissue, we analyzed histological samples obtained after surgery from patients with AAA. Patients' characteristics are shown in Tables II, III, and IV in the Data Supplement. We quantified the NET content and macrophage infiltration in the

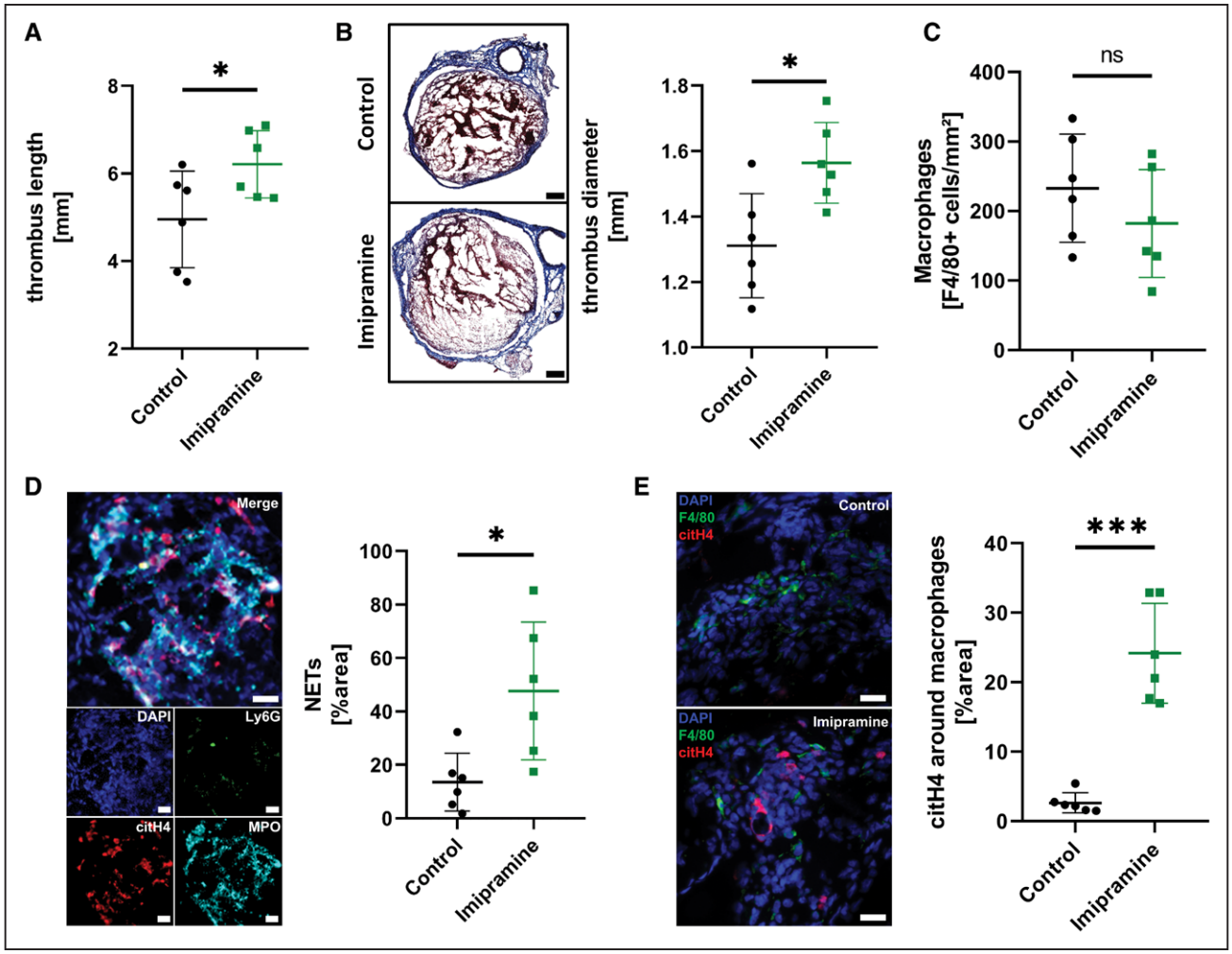

Figure 5. Inhibition of macropinocytosis in an in vivo murine thrombosis model leads to increased thrombus neutrophil extracellular trap (NET) burden and reduced thrombus resolution.
A, Thrombus length was assessed using a caliper. **B**, Frozen sections were stained using Masson Trichrome staining. The maximum diameter was measured using a virtual caliper built into the TissueFAXS software. A representative comparison is shown on the left side (×20 magnification, scale bar 200 µm). **C**, Macrophage density was quantified by fluorescence staining using an anti-F4/80 antibody. F4/80+ cells were measured using FIJI and cells per mm² were calculated. **D**, NETs were identified by fluorescence staining in sections of the thrombi using citrullinated histone 4 (citH4), myeloperoxidase (MPO), Ly6G and DAPI. A representative image of NETs is shown on the left side (×20 magnification, scale bar 20 µm). **E**, CitH4 was measured in macrophage-rich areas. A representative comparison of the 2 groups is shown on the left side (×20 magnification, scale bar 20 µm). For all subfigures: Data are given as mean±SD (n=6 per group, Shapiro-Wilk test, unpaired *t* test) ns indicates not significant, **P*<0.05, ****P*<0.001.

intraluminal thrombus as well as in the vessel wall by immunofluorescence staining of tissue specimens from 16 individual patients. We observed intense NET formation in the vessel wall of all 16 patients in our cohort. However, intraluminal thrombi were more heterogeneous. Most of the thrombi were not infiltrated by cells and did not contain any NETs (Figure VIIIA in the Data Supplement). NETs were identified by colocalization of citH4 with myeloperoxidase, CD177, and DAPI. Menders colocalization factor analysis revealed high colocalization of citH4 with all 3 other markers (mean M between 0.5 and 0.8 for all markers in vessel and thrombus, Figure VIIIB in the Data Supplement). Most NETs were found in the abluminal part, followed by the luminal part of the vessel wall with the least amount found in the thrombus (Figure 6A). When macrophage density was quantified between the different parts of the AAA, a similar picture was observed with most macrophages found at the abluminal site, and the lowest density of macrophages was seen in the thrombus (Figure VIIIC in the Data Supplement). In the thrombus, NET amounts correlated significantly with the number of infiltrating cells as shown in Figure VIIID in the Data Supplement. To evaluate the local NET amounts surrounding macrophages, nine 200×200 µm sized ROIs were randomly acquired per thrombus (Figure 6B) or vessel wall (Figure 6C) and scored for macrophage density ($CD68^{low}$, $CD68^{medium}$, and $CD68^{high}$). $CD68^{low}$ ROIs were associated with the highest surrounding NET signal in both thrombus and vessel wall. $CD68^{medium}$ and $CD68^{high}$ regions displayed lower amounts of NETs with a significant difference between $CD68^{medium}$ and $CD68^{high}$ ROIs in the vessel wall (Figure 6B and 6C).

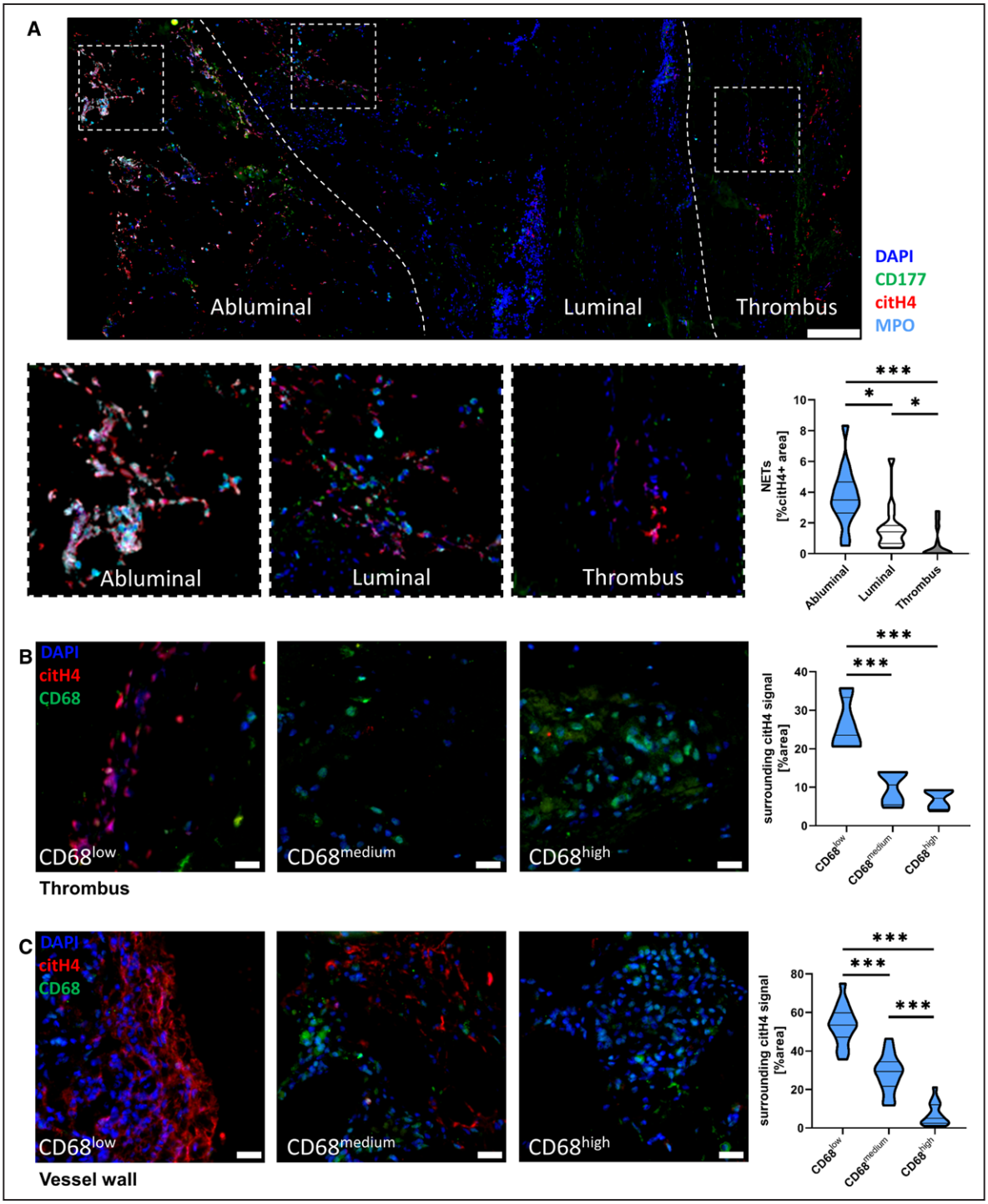

Figure 6. Local macrophage density is inversely associated with surrounding neutrophil extracellular trap (NET) amount in the thrombus and vessel wall of human abdominal aortic aneurysm (AAA).
A, NETs in AAA samples were stained by immunofluorescence against citrullinated histone 4 (citH4), myeloperoxidase (MPO), CD177, and DAPI. The left dashed line represents the approximate border between abluminal and luminal parts of the vessel wall, the right dashed line between the vessel wall and intraluminal thrombus (×20 magnification, scale bar 1 mm). Relative NET area was quantified as citH4+ areas. Data are given as percent citH4+ and are shown as violin plot of 16 patients for abluminal and luminal data and of 14 patients for the thrombi (D'Agostino-Pearson test, Kruskal-Wallis test with Benjamini-Krieger-Yekutieli false discovery rate). **B**, In thrombi with detectable NETs (>0.1% citH4), nine 200×200 µm sized regions of interest (ROIs) of the thrombus per patient were analyzed for their macrophage density and divided into $CD68^{low}$, $CD68^{medium}$, and $CD68^{high}$ areas. The relative citH4+ area was calculated in each ROI with FIJI. Data are represented as violin plot (scale bar 20 µm; n=4, Shapiro-Wilk test, 1-way ANOVA with Benjamini-Krieger-Yekutieli false discovery rate). **C**, Nine 200×200 µm sized ROIs of the abluminal part of the vessel wall per patient were analyzed for their macrophage density and divided into $CD68^{low}$, $CD68^{medium}$, and $CD68^{high}$ areas. The relative citH4+ area was calculated in each ROI with FIJI. Data are represented as violin plot (scale bar 20 µm; n=16, D'Agostino-Pearson test, 1-way ANOVA with Benjamini-Krieger-Yekutieli false discovery rate). *P<0.05 and ***P<0.001.

DISCUSSION

We here provide evidence that macrophages are capable to degrade and clear NETs by secreting DNases to cleave large fragments and by taking up the remaining extracellular DNA by endocytosis. We further showed that proinflammatory stimulation of macrophages primed the cells for enhanced degradation of NETs through a boost in macropinocytosis, leading to accelerated uptake and breakdown. When we inhibited macropinocytosis using imipramine in an in vivo murine thrombosis model, we found increased amounts of NETs inside the thrombus and a decreased resolution compared with the control group. Last, we demonstrated that increased macrophage density in AAA samples is inversely associated with the presence of NETs in the tissue.

To study the interaction of macrophages with extracellular DNA and NETs, we used an in vitro blood clot model.[26] Overall, all macrophage subsets were able to degrade NETs with increased uptake observed in proinflammatory macrophages. Our results are in accordance with previous reports showing that unpolarized macrophages were able to promote NET clearance.[23] Previous reports demonstrated that NET degradation of unpolarized macrophages was enhanced by adding DNase 1 to the NETs, preprocessing them into smaller fragments.[23] Our data showed that degradation of NETs by unpolarized and polarized macrophages and by their respective conditioned media, was inhibited by EDTA, a known inhibitor of DNase activity,[32] suggesting that even unpolarized macrophages produce and secrete DNases to allow breakdown of extracellular DNA. Candidates for DNases secreted by macrophages are DNase 1 and DNase 1L3.[22] These DNases are important regulators of NET formation and degradation as described previously.[22] Similar to previously published work, our data indicated that the main secreted form of DNase in macrophages is DNase 1L3.[41]

To characterize the repertoire of DNases in human macrophages, we analyzed cell lysates of unpolarized and polarized macrophages for the presence of DNase 1, DNase 1L1, DNase 1L3, DNase 2, and TREX 1. Long-term polarization increased intracellular DNase 1 amounts in M(lipopolysaccharide+IFN-γ). However, DNase 1 is also a potent regulator of actin polymerization and is found intracellularly as complex together with actin.[42,43] Consequently, we observed increased amounts of DNase 1:actin complexes in M(lipopolysaccharide+IFN-γ), which could be related to altered actin dynamics in M(lipopolysaccharide+IFN-γ) rather than intracellular DNA cleavage, as it was shown recently, that modulation of actin dynamics or targeting the specific binding of proteins to the cytoskeleton in macrophages could be used to selectively target individual macrophage subsets therapeutically.[44,45]

Our data also indicated that DNase 2 protein was increased after 24 hours in both polarized macrophage subsets. However, Farrera and Fadeel[23] and Lazzaretto and Fadeel[25] already demonstrated that knockdown of DNase 2 does not inhibit NET degradation by unpolarized macrophages and that cytoplasmic TREX 1 activity is needed for effective NET breakdown by macrophages. We did not observe changes in intracellular protein levels of TREX 1 as well as DNase 1L1 and DNase 1L3 upon polarization.

Upon intracellular activation of specific GTPases, macrophages can form cell surface protrusions, so-called filopodia, to spatially relocalize membrane-bound effector proteins onto these filopodia, altering, for example, their capacity to degrade the extracellular matrix.[10] Only DNase 1L1 has a signal sequence for membrane-anchoring through a GPI anchor,[46] and it was shown that human macrophages express DNase 1L1 on their surface.[47] Although we did not observe a difference in total intracellular amounts, interestingly M(lipopolysaccharide+IFN-γ) had increased colocalization of DNase 1L1 to their filopodia after 6 and 24 hours of polarization. This might, at least partially, explain an increase in NET degradation by proinflammatory macrophages.

Taken together, our DNase data suggest that altered intracellular DNase levels did not alone account for the increased breakdown of NETs by newly polarized M(lipopolysaccharide+IFN-γ). In addition, our data further indicated a rapid early acceleration of degradation in M(lipopolysaccharide+IFN-γ) rather than a constitutive increased degradation regulated through increased DNase protein amounts.

Consequently, we further characterized the mechanism of extracellular DNA uptake by macrophages. Preventing phagocytosis through inhibiting actin polymerization or phagosome-lysosome fusion reduced NET breakdown in our study significantly. We, therefore, suggest that NET degradation requires not only secreted DNases and extracellular breakdown of large DNA fragments into smaller entities but also an endocytic uptake. Previous reports suggested an activation of macropinocytosis after stimulation of toll-like receptors in macrophages.[48] In addition, macropinocytosis has been described to be altered in differently polarized macrophages.[49] Both lipopolysaccharide and granulocyte-macrophage colony-stimulating factor were demonstrated to boost macropinosome formation, leading to increased uptake of fluids as well as soluble proteins.[50] We show here that macropinocytosis was indeed increased for 2 hours after stimulation with lipopolysaccharide+IFN-γ in our in vitro generated macrophages. This early increase is followed by a late reduction to ≈50% of the baseline rate, similar to previous reports showing that continuous long-term polarization with lipopolysaccharide leads to dramatically reduced stimulated macropinocytosis in macrophages,[50] which might explain our observation that 24 hours prepolarized

M(lipopolysaccharide+IFN-γ) did not show increased degradation of NETs. Addition of imipramine, a selective inhibitor of macropinocytosis,[39] resulted in a selective reduction of NET breakdown in freshly stimulated proinflammatory macrophages. Therefore, we hypothesize that proinflammatory stimuli could prime macrophages not only for degradation of naked DNA or oligonucleotides but also for effective clearance of NETs.

In vivo effective clearance of extracellular DNA is necessary for the prevention of local inflammation and associated diseases.[51] Macrophages scavenge apoptotic cells as well as debris to restore the physiological integrity of tissue, protecting the organism from potential danger signals.[52] When we induced thrombosis through stenosis of the inferior vena cava in mice, we were able to show that macropinocytosis is necessary for the effective clearance of NETs in these thrombi. Inhibition of macropinocytosis by imipramine resulted in longer and wider thrombi with increased NET burden. When we analyzed the NET content of regions with high macrophage density, a significant NET reduction was seen in untreated animals compared with imipramine-treated animals, supporting our hypothesis, that macropinocytosis is an important pathway in the uptake of NETs by macrophages both in vitro as well as in vivo.

To investigate if similar processes might be seen in human disease, we obtained samples of AAA tissue from a cohort of patients who underwent surgery. NETs have been shown to play an important role in the pathogenesis of AAA and are thus prominently found in human samples.[20] AAAs are characterized through inflammation of the vessel wall with subsequent destruction of the medial layer and the formation of an intraluminal thrombus.[53] Monocytes are recruited to the vessel wall in AAA and differentiate into macrophages, which then polarize, depending on the disease state, into proinflammatory or anti-inflammatory subsets.[54,55] We showed that local macrophage density was negatively associated with surrounding NETs in the intraluminal thrombi as well as in the vessel wall. Therefore, we hypothesize that macrophages could also be involved in the removal of NETs in AAA.

In summary, we show here that macrophages degrade NETs in vitro by extracellular DNases and thus preprocess large NETs for subsequent intracellular uptake. Proinflammatory polarization leads to an increase in macropinocytosis, boosting the uptake of NETs by macrophages. Blocking of macropinocytosis in vivo in mice bearing a thrombus led to prolonged resolution with increased NET amounts inside the thrombus. In human AAA, macrophage density is inversely related to surrounding NETs. Taken together, by showing that polarization of macrophages impacts their ability to degrade NETs and by providing evidence that this ability critically depends on macropinocytosis in vitro and in vivo, we here describe, at least to the best of our knowledge, a novel aspect of NET degradation.

ARTICLE INFORMATION

Received January 23, 2020; accepted July 1, 2020.

Affiliations

From the Division of Cardiology, Department of Medicine II (P. Haider, J.B.K.-P., J.M., M.R., C.K., W.S.S., C.H., J.W., P. Hohensinner), Division of Vascular Surgery and Surgical Research Laboratories, Department of Surgery (C.B., W.E.), and Department of Blood Group Serology and Transfusion Medicine (M.B.F.), Medical University of Vienna, Austria; Ludwig Boltzmann Institute for Cardiovascular Research, Austria (J.B.K.-P., J.W.); Department of Biomedical Research, Danube University Krems, Austria (M.B.F.); Wilhelminenhospital, 3rd Department of Medicine, Cardiology and Intensive Care Medicine, Vienna, Austria (K.H.); Sigmund Freud University, Medical Faculty, Vienna, Austria (K.H.); and Medical University of Vienna, Core Facilities, Austria (J.W.).

Acknowledgments

P. Haider and P. Hohensinner planned the project; P. Haider performed the experiments and analyzed the results; J. B. Kral-Pointner performed the mouse surgeries; J. Mayer and M. Richter isolated and cultured macrophages; C. Kaun designed polymerase chain reaction (PCR) primers and performed RNA/cDNA generation; C. Brostjan and W. Eilenberg provided sections of abdominal aortic aneurysms and provided the demographic data for the cohort; M. B. Fischer provided leukocyte reduction chambers for the preparation of peripheral blood mononuclear cells (PBMCs) of healthy individuals; P. Haider wrote the article; J. B. Kral-Pointner, C. Hengstenberg, M.B. Fischer, W. S. Speidl, K. Huber, C. Brostjan, W. Eilenberg, J. Wojta, and P. Hohensinner edited the article and provided critical comments.

Sources of Funding

This project was supported by grants to J. Wojta and C. Brostjan from the Austrian Science Fund: SFB-F54.

Disclosures

None.

REFERENCES

1. Watanabe S, Alexander M, Misharin AV, Budinger GRS. The role of macrophages in the resolution of inflammation. *J Clin Invest*. 2019;129:2619–2628. doi: 10.1172/JCI124615
2. Murray PJ. Macrophage polarization. *Annu Rev Physiol*. 2017;79:541–566. doi: 10.1146/annurev-physiol-022516-034339
3. Mantovani A, Biswas SK, Galdiero MR, Sica A, Locati M. Macrophage plasticity and polarization in tissue repair and remodelling. *J Pathol*. 2013;229:176–185. doi: 10.1002/path.4133
4. Lim W, Gee K, Mishra S, Kumar A. Regulation of B7.1 costimulatory molecule is mediated by the IFN regulatory factor-7 through the activation of JNK in lipopolysaccharide-stimulated human monocytic cells. *J Immunol*. 2005;175:5690–5700. doi: 10.4049/jimmunol.175.9.5690
5. Gordon S, Plüddemann A. Tissue macrophages: heterogeneity and functions. *BMC Biol*. 2017;15:53.
6. Murray PJ, Allen JE, Biswas SK, Fisher EA, Gilroy DW, Goerdt S, Gordon S, Hamilton JA, Ivashkiv LB, Lawrence T, et al. Macrophage activation and polarization: nomenclature and experimental guidelines. *Immunity*. 2014;41:14–20. doi: 10.1016/j.immuni.2014.06.008
7. Thaler B, Baik N, Hohensinner PJ, Baumgartner J, Panzenböck A, Stojkovic S, Demyanets S, Huk I, Rega-Kaun G, Kaun C, et al. Differential expression of Plg-RKT and its effects on migration of proinflammatory monocyte and macrophage subsets. *Blood*. 2019;134:561–567. doi: 10.1182/blood.2018850420
8. Thaler B, Hohensinner PJ, Baumgartner J, Haider P, Krychtiuk KA, Schörgenhofer C, Jilma B, Hell L, Fischer MB, Huber K, et al. Protease-activated receptors 1 and 3 are differentially expressed on human monocyte subsets and are upregulated by lipopolysaccharide ex vivo and in vivo. *Thromb Haemost*. 2019;119:1394–1402. doi: 10.1055/s-0039-1692219

9. Newby AC. Metalloproteinase expression in monocytes and macrophages and its relationship to atherosclerotic plaque instability. *Arterioscler Thromb Vasc Biol.* 2008;28:2108–2114. doi: 10.1161/ATVBAHA.108.173898
10. Hohensinner PJ, Baumgartner J, Kral-Pointner JB, Uhrin P, Ebenbauer B, Thaler B, Doberer K, Stojkovic S, Demyanets S, Fischer MB, et al. PAI-1 (Plasminogen Activator Inhibitor-1) expression renders alternatively activated human macrophages proteolytically quiescent. *Arterioscler Thromb Vasc Biol.* 2017;37:1913–1922. doi: 10.1161/ATVBAHA.117.309383
11. Hohensinner PJ, Mayer J, Kichbacher J, Kral-Pointner J, Thaler B, Kaun C, Hell L, Haider P, Mussbacher M, Schmid JA, et al. Alternative activation of human macrophages enhances tissue factor expression and production of extracellular vesicles [published online January 23, 2020]. *Haematologica.* doi: 10.3324/haematol.2019.220210
12. Murray PJ, Wynn TA. Protective and pathogenic functions of macrophage subsets. *Nat Rev Immunol.* 2011;11:723–737. doi: 10.1038/nri3073
13. Mendoza-Coronel E, Ortega E. Macrophage polarization modulates FcγR- and CD13-mediated phagocytosis and reactive oxygen species production, independently of receptor membrane expression. *Front Immunol.* 2017;8:303. doi: 10.3389/fimmu.2017.00303
14. Gordon S, Plüddemann A. Macrophage clearance of apoptotic cells: a critical assessment. *Front Immunol.* 2018;9:127.
15. Brinkmann V, Reichard U, Goosmann C, Fauler B, Uhlemann Y, Weiss DS, Weinrauch Y, Zychlinsky A. Neutrophil extracellular traps kill bacteria. *Science.* 2004;303:1532–1535. doi: 10.1126/science.1092385
16. Martinod K, Wagner DD. Thrombosis: tangled up in NETs. *Blood.* 2014;123:2768–2776. doi: 10.1182/blood-2013-10-463646
17. Fuchs TA, Brill A, Duerschmied D, Schatzberg D, Monestier M, Myers DD Jr, Wrobleski SK, Wakefield TW, Hartwig JH, Wagner DD. Extracellular DNA traps promote thrombosis. *Proc Natl Acad Sci USA.* 2010;107:15880–15885. doi: 10.1073/pnas.1005743107
18. Hisada Y, Grover SP, Maqsood A, Houston R, Ay C, Noubouossie DF, Cooley BC, Wallén H, Key NS, Thålin C, et al. Neutrophils and neutrophil extracellular traps enhance venous thrombosis in mice bearing human pancreatic tumors. *Haematologica.* 2020;105:218–225. doi: 10.3324/haematol.2019.217083
19. Silvestre-Roig C, Braster Q, Wichapong K, Lee EY, Teulon JM, Berrebeh N, Winter J, Adrover JM, Santos GS, Froese A, et al. Externalized histone H4 orchestrates chronic inflammation by inducing lytic cell death. *Nature.* 2019;569:236–240. doi: 10.1038/s41586-019-1167-6
20. Meher AK, Spinosa M, Davis JP, Pope N, Laubach VE, Su G, Serbulea V, Leitinger N, Ailawadi G, Upchurch GR Jr. Novel Role of IL (Interleukin)-1β in neutrophil extracellular trap formation and abdominal aortic aneurysms. *Arterioscler Thromb Vasc Biol.* 2018;38:843–853. doi: 10.1161/ATVBAHA.117.309897
21. Thålin C, Hisada Y, Lundström S, Mackman N, Wallén H. Neutrophil extracellular traps: villains and targets in arterial, venous, and cancer-associated thrombosis. *Arterioscler Thromb Vasc Biol.* 2019;39:1724–1738. doi: 10.1161/ATVBAHA.119.312463
22. Jiménez-Alcázar M, Rangaswamy C, Panda R, Bitterling J, Simsek YJ, Long AT, Bilyy R, Krenn V, Renné C, Renné T, et al. Host DNases prevent vascular occlusion by neutrophil extracellular traps. *Science.* 2017;358:1202–1206. doi: 10.1126/science.aam8897
23. Farrera C, Fadeel B. Macrophage clearance of neutrophil extracellular traps is a silent process. *J Immunol.* 2013;191:2647–2656. doi: 10.4049/jimmunol.1300436
24. Nakazawa D, Shida H, Kusunoki Y, Miyoshi A, Nishio S, Tomaru U, Atsumi T, Ishizu A. The responses of macrophages in interaction with neutrophils that undergo NETosis. *J Autoimmun.* 2016;67:19–28. doi: 10.1016/j.jaut.2015.08.018
25. Lazzaretto B, Fadeel B. Intra- and extracellular degradation of neutrophil extracellular traps by macrophages and dendritic cells. *J Immunol.* 2019;203:2276–2290. doi: 10.4049/jimmunol.1800159
26. Pfaffenberger S, Devcic-Kuhar B, Kollmann C, Kastl SP, Kaun C, Speidl WS, Weiss TW, Demyanets S, Ullrich R, Sochor H, et al. Can a commercial diagnostic ultrasound device accelerate thrombolysis? An in vitro skull model. *Stroke.* 2005;36:124–128. doi: 10.1161/01.STR.0000150503.10480.a7
27. Brill A, Fuchs TA, Chauhan AK, Yang JJ, De Meyer SF, Köllnberger M, Wakefield TW, Lämmle B, Massberg S, Wagner DD. von Willebrand factor-mediated platelet adhesion is critical for deep vein thrombosis in mouse models. *Blood.* 2011;117:1400–1407. doi: 10.1182/blood-2010-05-287623
28. Reagan-Shaw S, Nihal M, Ahmad N. Dose translation from animal to human studies revisited. *FASEB J.* 2008;22:659–661. doi: 10.1096/fj.07-9574LSF
29. Schindelin J, Arganda-Carreras I, Frise E, Kaynig V, Longair M, Pietzsch T, Preibisch S, Rueden C, Saalfeld S, Schmid B, et al. Fiji: an open-source platform for biological-image analysis. *Nat Methods.* 2012;9:676–682. doi: 10.1038/nmeth.2019
30. Hohensinner PJ, Baumgartner J, Ebenbauer B, Thaler B, Fischer MB, Huber K, Speidl WS, Wojta J. Statin treatment reduces matrix degradation capacity of proinflammatory polarized macrophages. *Vascul Pharmacol.* 2018;110:49–54. doi: 10.1016/j.vph.2018.08.003
31. Rega-Kaun G, Ritzel D, Kaun C, Ebenbauer B, Thaler B, Prager M, Demyanets S, Wojta J, Hohensinner PJ. Changes of circulating extracellular vesicles from the liver after roux-en-y bariatric surgery. *Int J Mol Sci.* 2019;20:2153.
32. Barra GB, Santa Rita TH, de Almeida Vasques J, Chianca CF, Nery LF, Santana Soares Costa S. EDTA-mediated inhibition of DNases protects circulating cell-free DNA from ex vivo degradation in blood samples. *Clin Biochem.* 2015;48:976–981. doi: 10.1016/j.clinbiochem.2015.02.014
33. Guéroult M, Picot D, Abi-Ghanem J, Hartmann B, Baaden M. How cations can assist DNase I in DNA binding and hydrolysis. *PLoS Comput Biol.* 2010;6:e1001000. doi: 10.1371/journal.pcbi.1001000
34. Chhabra D, Bao S, dos Remedios CG. The distribution of cofilin and DNase I in vivo. *Cell Res.* 2002;12:207–214. doi: 10.1038/sj.cr.7290126
35. McNiven MA. Breaking away: matrix remodeling from the leading edge. *Trends Cell Biol.* 2013;23:16–21. doi: 10.1016/j.tcb.2012.08.009
36. Shiokawa D, Matsushita T, Shika Y, Shimizu M, Maeda M, Tanuma S. DNase X is a glycosylphosphatidylinositol-anchored membrane enzyme that provides a barrier to endocytosis-mediated transfer of a foreign gene. *J Biol Chem.* 2007;282:17132–17140. doi: 10.1074/jbc.M610428200
37. Casella JF, Flanagan MD, Lin S. Cytochalasin D inhibits actin polymerization and induces depolymerization of actin filaments formed during platelet shape change. *Nature.* 1981;293:302–305. doi: 10.1038/293302a0
38. Gordon AH, Hart PD, Young MR. Ammonia inhibits phagosome-lysosome fusion in macrophages. *Nature.* 1980;286:79–80. doi: 10.1038/286079a0
39. Lin HP, Singla B, Ghoshal P, Faulkner JL, Cherian-Shaw M, O'Connor PM, She JX, Belin de Chantemele EJ, Csányi G. Identification of novel macropinocytosis inhibitors using a rational screen of Food and Drug Administration-approved drugs. *Br J Pharmacol.* 2018;175:3640–3655. doi: 10.1111/bph.14429
40. Yan H, Zhou HF, Akk A, Hu Y, Springer LE, Ennis TL, Pham CTN. Neutrophil proteases promote experimental abdominal aortic aneurysm via extracellular trap release and plasmacytoid dendritic cell activation. *Arterioscler Thromb Vasc Biol.* 2016;36:1660–1669. doi: 10.1161/ATVBAHA.116.307786
41. Wilber A, Lu M, Schneider MC. Deoxyribonuclease I-like III is an inducible macrophage barrier to liposomal transfection. *Mol Ther.* 2002;6:35–42. doi: 10.1006/mthe.2002.0625
42. Mannherz HG, Leigh JB, Leberman R, Pfrang H. A specific 1:1 G-actin:DNAase i complex formed by the action of DNAase I on F-actin. *FEBS Lett.* 1975;60:34–38. doi: 10.1016/0014-5793(75)80412-1
43. Hitchcock SE, Carisson L, Lindberg U. Depolymerization of F-actin by deoxyribonuclease I. *Cell.* 1976;7:531–542. doi: 10.1016/0092-8674(76)90203-8
44. Pergola C, Schubert K, Pace S, Ziereisen J, Nikels F, Scherer O, Hüttel S, Zahler S, Vollmar AM, Weinigel C, et al. Modulation of actin dynamics as potential macrophage subtype-targeting anti-tumour strategy. *Sci Rep.* 2017;7:41434. doi: 10.1038/srep41434
45. Bandaru S, Ala C, Salimi R, Akula MK, Ekstrand M, Devarakonda S, Karlsson J, Van den Eynden J, Bergström G, Larsson E, et al. Targeting filamin a reduces macrophage activity and atherosclerosis. *Circulation.* 2019;140:67–79. doi: 10.1161/CIRCULATIONAHA.119.039697
46. Keyel PA. Dnases in health and disease. *Dev Biol.* 2017;429:1–11. doi: 10.1016/j.ydbio.2017.06.028
47. Mohan Kumar D, Yamaguchi M, Miura K, Lin M, Los M, Coy JF, Rikihisa Y. Ehrlichia chaffeensis uses its surface protein EtpE to bind GPI-anchored protein DNase X and trigger entry into mammalian cells. *PLoS Pathog.* 2013;9:e1003666. doi: 10.1371/journal.ppat.1003666
48. Luo L, Wall AA, Tong SJ, Hung Y, Xiao Z, Tarique AA, Sly PD, Fantino E, Marzolo MP, Stow JL. TLR crosstalk activates LRP1 to recruit Rab8a and PI3Kγ for suppression of inflammatory responses. *Cell Rep.* 2018;24:3033–3044. doi: 10.1016/j.celrep.2018.08.028
49. Doodnauth SA, Grinstein S, Maxson ME. Constitutive and stimulated macropinocytosis in macrophages: roles in immunity and in the pathogenesis of atherosclerosis. *Philos Trans R Soc Lond B Biol Sci.* 2019;374:20180147. doi: 10.1098/rstb.2018.0147
50. Redka DS, Gütschow M, Grinstein S, Canton J. Differential ability of proinflammatory and anti-inflammatory macrophages to perform macropinocytosis. *Mol Biol Cell.* 2018;29:53–65. doi: 10.1091/mbc.E17-06-0419

51. Daniel C, Leppkes M, Muñoz LE, Schley G, Schett G, Herrmann M. Extracellular DNA traps in inflammation, injury and healing. *Nat Rev Nephrol.* 2019;15:559–575. doi: 10.1038/s41581-019-0163-2
52. Binder CJ, Papac-Milicevic N, Witztum JL. Innate sensing of oxidation-specific epitopes in health and disease. *Nat Rev Immunol.* 2016;16:485–497. doi: 10.1038/nri.2016.63
53. Kuivaniemi H, Ryer EJ, Elmore JR, Tromp G. Understanding the pathogenesis of abdominal aortic aneurysms. *Expert Rev Cardiovasc Ther.* 2015;13:975–987. doi: 10.1586/14779072.2015.1074861
54. Boytard L, Spear R, Chinetti-Gbaguidi G, Acosta-Martin AE, Vanhoutte J, Lamblin N, Staels B, Amouyel P, Haulon S, Pinet F. Role of proinflammatory CD68(+) mannose receptor(-) macrophages in peroxiredoxin-1 expression and in abdominal aortic aneurysms in humans. *Arterioscler Thromb Vasc Biol.* 2013;33:431–438. doi: 10.1161/ATVBAHA.112.300663
55. Raffort J, Lareyre F, Clément M, Hassen-Khodja R, Chinetti G, Mallat Z. Monocytes and macrophages in abdominal aortic aneurysm. *Nat Rev Cardiol.* 2017;14:457–471. doi: 10.1038/nrcardio.2017.52